

Special topic paper

Shaoyan Fan, Koki Nasu, Yukio Takeuchi, Miho Fukuda, Hirotugu Arai, Keisuke Taniguchi and Yuichi Onda*

Transport of radioactive materials from terrestrial to marine environments in Fukushima over the past decade

<https://doi.org/10.1515/pac-2023-0802>

Abstract: While 20 % of radionuclides released from the Fukushima Daiichi Nuclear Power Plant accident had been deposited in the terrestrial environment, rivers remain the long-term source for ^{137}Cs , primarily through particulate transfer, from terrestrial to marine ecosystems. In this study, we estimated the suspended ^{137}Cs flux to the ocean at 11 sites in the coastal area between October 2012 and December 2020 to be 17 TBq, based on our long-term monitoring data of concentrations of suspended ^{137}Cs and suspended solids. The cumulative loss of suspended ^{137}Cs from each site to the ocean ranged from 0.1 % to 1.7 % of initial deposition throughout the observation period, depending on the effect of dam lakes and normalized river discharge. The higher loss is also thought to be the large outflow of runoff during the typhoon. The current level of the suspended ^{137}Cs concentrations was lowered to 1/10–1/100 of those immediately after the accident. The average value of the decreasing trend for each site was approximated using the equation: $y = a_1 e^{-k_1 t} + a_2 e^{-k_2 t}$. The rate constant k_1 is higher in areas with intensive land use, such as pastures, bare land, and water surfaces, and k_2 is lower in urban areas.

Keywords: cesium; Fukushima; river.

Introduction

The magnitude 9.0 earthquake and tsunami caused by the Great East Japan Earthquake on March 11, 2011, caused a severe accident at TEPCO's Fukushima Daiichi Nuclear Power Plant (FDNPP), releasing large amounts of cesium-137 (^{137}Cs) and other radionuclides [1, 2]. It is estimated that approximately 20 % (2.7 PBq) of the ^{137}Cs released into the atmosphere was deposited on the land area of the Fukushima Prefecture [3], with approximately 67 % (1.8 PBq) of this was reported to have been deposited in the forests [3], which account for about 71 % of the total area of the Fukushima Prefecture [4]. Estimating the amount of ^{137}Cs that migrated to the ocean via rivers is important to understand the amount of ^{137}Cs discharged from the terrestrial to the marine environments.

The transported form of ^{137}Cs in rivers is either dissolved in water as ions (dissolved form) or absorbed by soil particles (suspended form) [5, 6]. According to previous surveys of rivers in the Fukushima Prefecture, the suspended form ^{137}Cs account for 84–92 % of the ^{137}Cs in the Abukuma River from August 2011 to May 2012 [7], and more than 96 % in the rivers from June 2011 to August 2015 [8]. It has also been reported that more than 90 % of the ^{137}Cs that migrated during the three large runoffs in 2019–2020 was in suspended form [9]. In addition, the

*Corresponding author: Yuichi Onda, Center for Research in Radiation, Isotopes and Earth System Sciences, University of Tsukuba, 1-1-1 Tennodai, Tsukuba, 305-8572, Japan, e-mail: onda@geoenv.tsukuba.ac.jp

Shaoyan Fan, Koki Nasu, Yukio Takeuchi and Miho Fukuda, Fukushima Prefectural Centre for Environmental Creation, 10-2 Fukasaku, Miharu, Fukushima, 963-7700, Japan

Hirotugu Arai, Center for Ecological Research, Kyoto University, 2-509-3 Hirano, Otsu, Shiga, 520-2113, Japan

Keisuke Taniguchi, National Institute of Technology, Tsuyama College, 624-1 Numa, Tsuyama-City, Okayama, 708-8509, Japan

results of ^{137}Cs dissolution tests using seawater indicated that 2.8–6.6 % of the ^{137}Cs in suspended solids was released into seawater, suggesting that suspended ^{137}Cs may contribute to increasing concentrations of dissolved ^{137}Cs in the ocean [10]. Therefore, evaluation of suspended ^{137}Cs is important for understanding the changes in ^{137}Cs concentrations in rivers and the amount of ^{137}Cs transferred to the sea.

Observations from the time of the accident to 2015 suggest that most of the ^{137}Cs remained near the ground surface in forest, and the annual amount of ^{137}Cs migrating out of forested areas was less than 0.3 % of the initial deposition, suggesting that most of the deposited ^{137}Cs remained within forest ecosystems [3]. ^{137}Cs is thought to be discharged into the ocean via rivers, mainly in suspended form, owing to rainfall and other factors. It has also been reported that the suspended ^{137}Cs flux is strongly influenced by the amount and intensity of precipitation during rainfall [11]. The suspended ^{137}Cs flux from Typhoon No. 15 in 2011, which struck immediately after the accident, was reported to be 6.2 TBq which accounted for 61 % of the suspended ^{137}Cs flux from August 2011 to May 2012 [7]. In October 2019, the Fukushima Prefecture was hit by a natural disaster associated with a large-scale outflow of water, and a large amount of ^{137}Cs was discharged from the terrestrial to the marine environments [10]. The results of the 10-year observation of ^{137}Cs in river ecosystem, including these previous studies, can be regarded to be the response to the effects of decontamination work in the upstream areas of the observation sites and the gradual lifting of the “difficult to return zone”, which was implemented from July 2012 to March 2017. On the other hand, the results from 2017 onward are considered to be the observation results affected by normal human activities after the completion of “area-wide decontamination”, except for the “difficult to return zone”. Twelve years have passed since the accident. Air dose rates in paddy fields, fields, and urban areas (PFU) have decreased sufficiently, evacuation order areas have been lifted, and residents have returned. Evacuation orders were also lifted by May 2023 in specific reconstruction and revitalization centers in six municipalities in difficult-to-return zones (<https://www.pref.fukushima.lg.jp/site/portal-english/en03-08.html>). In areas outside of the return zones, decontamination work was completed in 2018, but it is believed that approximately 90 % of the amount of initial deposition remains in forested areas that have not yet been decontaminated. Temporal changes in suspended ^{137}Cs concentrations and transport fluxes of suspended ^{137}Cs by rivers flowing into the ocean have become increasingly important, especially in the Hamadori region of the Fukushima Prefecture.

Therefore, this study aimed to understand the dynamics of ^{137}Cs transported to the ocean via rivers based on the results of long-term evaluation of suspended ^{137}Cs concentrations, suspended solids (SS), and river discharge by the University of Tsukuba (2011–2015) and the Fukushima Prefectural Center for Environmental Creation (2015–). The amount of ^{137}Cs transported from the inland area of the Fukushima Prefecture to the ocean from October 2012 to December 2020 was calculated and used to analyze the impact of ^{137}Cs discharge on the ocean.

Materials and methods

In this study, data from 11 monitoring sites located within 80 km of the FDNPP in the downstream areas of nine rivers (Abukuma, Mano, Nitta, Ota, Odaka, Ukedo, Asami, Fujiwara, and Same) in the Fukushima Prefecture (Fig. 1) were used for assessments. Eleven sites were selected from those described by Taniguchi et al. (2019) [8]: Nos. 6, 8, 9, 10, 15, 23, 24, 25, 27, 28, and 29. The coordinates of each site are listed in Table 1 and their locations are shown in Fig. 1. Iwanuma (Iwa), located in the lower reaches of the Abukuma River, is the only one of the 11 sites located in the Miyagi Prefecture, whereas the other 10 sites are located 1–8 km from the mouth of the river on the coast of the Fukushima Prefecture.

The Abukuma River is classified as a class A, and the other eight rivers are classified as class B based on the Japan River Law (https://www.mlit.go.jp/river/basic_info/english/admin.html). These rivers discharge directly into the ocean. The catchment area of Iwanuma (Iwa) is the largest at 5313.2 km², and the other catchment areas are as follows: Ojimadazeiki (Oji) 110.8 km², Haramachi (Har) 200.3 km², Kitamachi (Kit) 35.8 km², Ota (Ota) 49.9 km², Odaka (Oda) 50.3 km², Ukedo (Uke) 152.6 km², Takase (Tak) 263.7 km², Asami (Asa) 25.8 km², Onahama (Ona) 70.1 km², and Matsubara (Mat) 570.9 km² (Table 1). The relative altitude in each basin ranges from 624 m to 1975 m and the average slope of the basin ranges from 10.2° to 19.5° (Table 1). No significant geographical differences were observed between the basins.

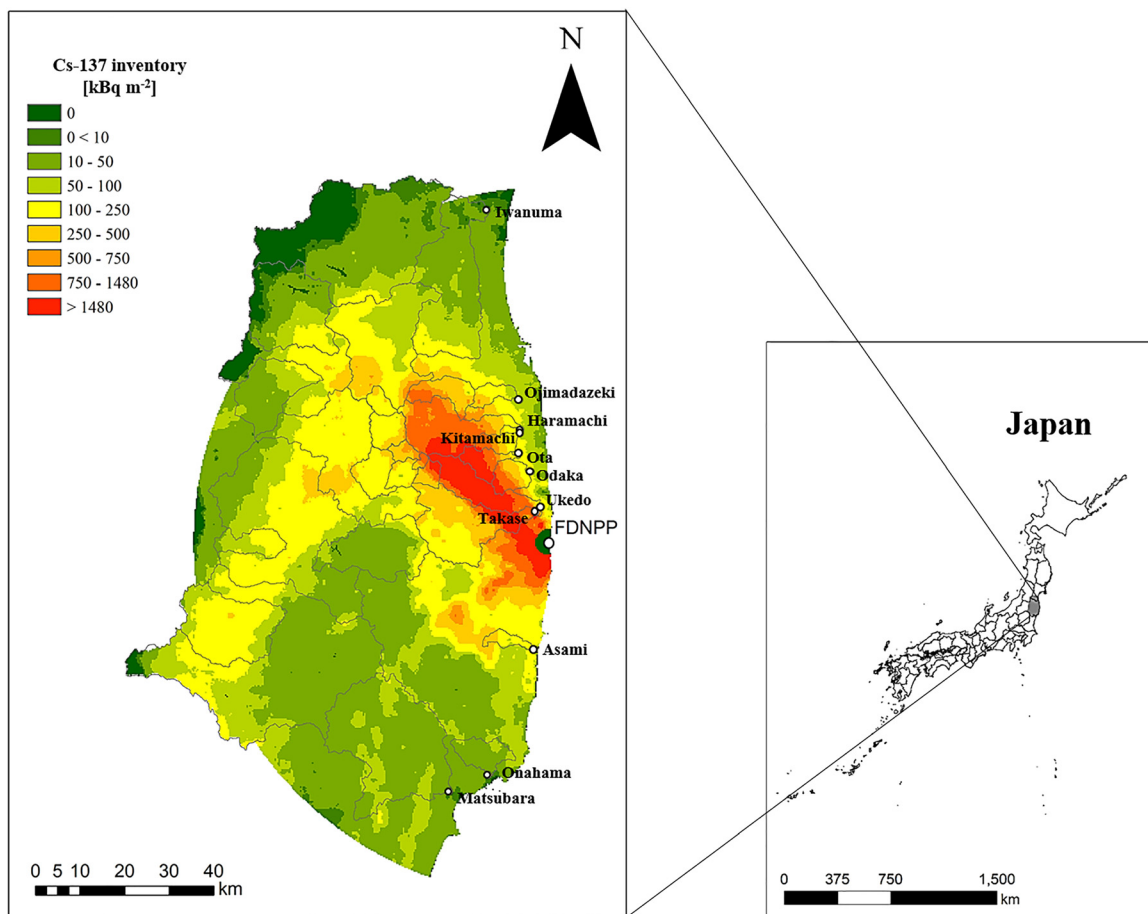


Fig. 1: River monitoring stations. Detailed description is shown in Table 1. The color contours in the background of the map show the ^{137}Cs deposition as of July 2011.

Seven river observation sites (Har, Kit, Ota, Oda, Uke, Tak, and Asa) were located in areas where evacuation orders had previously been issued. Har, Kit, Ota, and Asa lifted the emergency evacuation preparation zone designation on September 30, 2011. Subsequently, the restriction on residency at Oda was lifted in July 2016, and the Uke and Tak, located within the town of Namie, lifted their restrictions on March 31, 2017.

Collection of suspended solids in river and concentration of suspended ^{137}Cs

Suspended solids (SS) in the river were collected using a time-integrated suspended solid sampler [12]. The sampler was positioned 0.2–5 m from the river edge and 5–20 cm from the riverbed, so that it always remained below the water surface, and its position was adjusted depending on the location. Suspended solid samples were collected every few days or months. The suspended sediment in the sampler was returned to the laboratory and allowed to stand for one week. Following this settling period, the supernatant was discarded and the remaining suspension was dried. For SS samples collected from June 2011 to November 2017, drying was carried out in a dryer at 105–110 °C for at least 24 h, while SS samples collected after December 2017 were dried in a lyophilizer under vacuum for at least 24 h. The dried SS samples were then analyzed using high-purity germanium semiconductor detectors (Canberra-Eurisys GC2018, GC4020, Ortec GEM20-70, GEM30-70, GMX30-70-HJ, and GWL-150-16-LB-WWT-HJ-S) at with a measurement of 3600s, 7200s, 10800s. Target errors were set to ± 1 sigma ($\mu \pm \sigma$). The suspended ^{137}Cs concentration [$\text{Cs}_{\text{s}} (\text{Bq kg}^{-1})$] was then calculated.

Table 1: Site characteristics and time-dependent parameters of ^{137}Cs .

Site name (abbreviation)	River name (River system)	Latitude	Longitude	Relative altitude	Average slope	S deposition density [kBq m ⁻²]	Deposition amount [Bq]	Coverage of Dam [%]	$T_{\text{eff_total}}$	$T_{\text{eff_1}}$	$T_{\text{eff_1}}^{\#}$	$T_{\text{eff_2}}$	Decreasing trend $y = a_1 e^{k_1 t} + a_2 e^{k_2 t}$	k_1	k_2
Iwanuma (Iwa)	Abukuma (Abukuma)	140°52'	38°0'54.1"	1975	13.2	5313.2	88.4	4.70×10^{14}	13.9	307 ± 0.38	1.75 ± 0.41	1.47	$11.55 \pm 9.95^{\text{a}}$	2.79	0.29
Ojimadazeki (Oji)	Mano (Mano)	140°57'	37°42'42"	694	16.9	110.8	405.5	4.49×10^{13}	60.9	2.59 ± 0.22	2.54 ± 0.71	4.61	2.84 ± 0.78	5.57	0.21
Haramachi (Har)	Niida (Niida)	140°57'	37°39'4"	898	14.4	200.3	963.7	1.93×10^{14}	0.0	2.19 ± 0.19	2.39 ± 0.50	2.97	$4.75 \pm 3.16^{\text{a}}$	6.7	0.29
Kitamachi (Kit)	Mizunashi (Niida)	140°57"	37°38'40"	624	14.9	35.8	564.5	2.02×10^{13}	34.9	2.18 ± 0.15	1.37 ± 0.16	1.45	2.66 ± 0.48	19.80	0.32
Ota (Ota)	Ota (Ota)	140°57'	37°36'12"	695	19.5	49.9	1767.5	8.82×10^{13}	90	2.36 ± 0.26	3.32 ± 1.41	3.82	2.77 ± 1.07	4.96	0.27
Odaka (Oda)	Odaka (Odaka)	140°59'1"	37°33'58"	499	10.2	50.3	724.2	3.64×10^{13}	0.00	3.38 ± 0.60	3.49 ± 1.72 ^a	11.36	2.41 ± 0.99	7.35	0.14
Ukedo (Uke)	Ukedo (Ukedo)	141°0'	37°29'41"	1037	15.4	152.6	2565.9	3.92×10^{14}	61.1	2.95 ± 0.32	2.61 ± 0.55	2.77	2.33 ± 0.61	6.32	0.21
Takase (Tak)	Takase (Ukedo)	140°59'	37°29'7"	1048	16.3	263.7	726.0	1.91×10^{14}	0.0	3.28 ± 0.57	1.69 ± 0.26	1.69	$9.87 \pm 15.90^{\text{a}}$	0.68	0.00
Asami (Asa)	Asami (Asami)	140°59'	37°12'20"	863	18.3	25.8	193.8	5.00×10^{12}	0.0	2.45 ± 0.38	2.05 ± 0.75	2.05	$5.92 \pm 7.94^{\text{a}}$	7.36	0.26
Onahama (Ona)	Fujiwara (Fujiwara)	140°52'	36°57'03"	659	10.7	70.1	38.8	2.72×10^{12}	0.0	5.45 ± 1.19	1.86 ± 0.35	2.12	– ^a	0.69	0.00
Matsubara (Mat)	Same (Same)	140°46'	36°55'03"	871	18.0	570.9	40.0	2.28×10^{13}	89.3	3.55 ± 0.74	3.27 ± 1.65 ^a	3.73	$4.47 \pm 3.19^{\text{a}}$	10.11	0.18
			43"												

$T_{\text{eff_total}}$ is 1.7–10 years after the accident; $T_{\text{eff_1}}$ is 1.7–5.08 years after the accident [8]; $T_{\text{eff_2}}$ is 5.08–10 years after the accident. Relative altitude is the difference in elevation between the highest and lowest points in the watershed. ^aMeans unsignificant statistically.

All data were decay-corrected to the date of sample collection. The suspended ^{137}Cs concentrations from June 2011 to March 2021, along with other initial data, are available at the CRiED database site [13,14,15] and in a Scientific Data paper [16]. In this study, we used the values remeasured from these data with a well-type germanium semiconductor detector (GWL-150-16-LB-AWT-HJ-S from ORTEC) for samples collected with less than 0.1 g of sediment (samples collected at Odaka [Oda] on April 8, 2016).

Observation of water level and turbidity

SS samplers were installed near observation points included in the Ministry of Land, Infrastructure, Transport, and Tourism's Hydrologic Water Quality Database (<http://www1.river.go.jp/>) and the Fukushima Prefecture Integrated River Basin Information System (<https://kaseninf.pref.fukushima.jp/gis/>) at 10 sites (excluding Kitamachi). Water level data recorded in these databases were used for the analysis. For Kitamachi, data obtained from a pressure-type water level gauge (Rugged TROLL 100, *In Situ* Inc.) installed at approximately the same location as the SS sampler were used. In both cases, the water level data were recorded every 10 min. Turbidity data were obtained every 10 min using turbidity meters (Analyte Turbidity Meter 3000-NTU by MacVan, TC3000 by OPTEX, and INFINITY-CLW, JFE Advantech) installed at all locations.

Calculation of river discharge Q

The recorded water level data were converted into river discharge data using the quadratic $h\text{-}Q$ equation (h : water level, Q : discharge) obtained from discharge observations. The $h\text{-}Q$ equation for the Iwanuma site was developed by the Ministry of Land, Infrastructure, Transport, and Tourism, and the $h\text{-}Q$ equations for the Mat, Ona, Oda, Uke, Tak, and Har sites were developed annually by the Fukushima Prefecture. The $h\text{-}Q$ equations for the Oji, Kit, Ota, and Asa sites were not developed by the Fukushima Prefecture; therefore, the $h\text{-}Q$ equations developed by the authors based on flow observations were used. The Ministry of Land, Infrastructure, Transport and Tourism and Fukushima Prefecture conduct observations twice a month (24 times a year) during normal water flow and intensive flow observation during flooding to calculate the $h\text{-}Q$ equation for each year. Observations during outflow are aimed at the highest annual water level, but in the case of the Fukushima Prefecture, the number of outflow observations is limited to once a year, so there are cases where outflow observations cannot be made, or the outflow that reaches the maximum water level is missed. The authors conducted flow observations once or twice a year during normal water flow and once or twice a year during outflow observation and recreated the $h\text{-}Q$ equation every few years based on the presence or absence of riverbed fluctuations caused by large outflows.

When water-level data could not be obtained for a long period because of time due to the absence of a water-level station or river construction near a water-level station, a linear conversion formula ($Q\text{-}Q$ formula) was created to estimate the flow rate at the missing location from the flow rates of other rivers in the vicinity to compensate for the flow rate during the missing period. For example, water level data from the water level station at the Ota site in 2020 exhibited fluctuations unrelated to the rainfall and flow observations. A conversion formula was created to determine the flow rate at the Ota station from the flow rate at a nearby Oda station, which was used as the flow rate for this period. In addition, there was a loss of water level data from October 16 to 30, 2022, owing to equipment replacement work at the Har water level station; however, this was supplemented using the $Q\text{-}Q$ equation between the flow rate at Tak and the flow rate at Har in the same year. The Tak site was selected because it was close to the Har site and was an observation site with no dams in the basin. The equations used for the completion and period of application are shown in Supplementary material Table 1.

Calculation of SS concentration

Turbidity data were converted to suspended solid concentration (SSC) data using a first-order conversion equation developed for each sensor using test samples of known concentrations. The test samples were prepared from the bottom mud of the Horai Dam, located in the middle reaches of the Abukuma River [17]. Valid turbidity data may not have been obtained because of sensor burial, malfunction, or contamination. In such cases, linear conversion equations between the SS concentration and flow rate were developed and supplemented by estimating the SSC from the flow rate Q . The conversion equations are shown in Supplementary material Table 2.

Calculation of the amount of suspended ^{137}Cs

The activity flow rate of ^{137}Cs in suspended form, l [Bq s^{-1}], was calculated using the concentration of suspended ^{137}Cs , C_{ss} [Bq kg^{-1}], suspended solid concentration, SSC [kg m^{-3}], and river flow rate, Q [$\text{m}^3 \text{s}^{-1}$], as follows:

$$l = C_{\text{ss}} \times Q \times \text{SSC} \quad (1)$$

The flow rate of ^{137}Cs transported were summed monthly to obtain the monthly flux of ^{137}Cs transported in suspended form L_{month} . The cumulative loss of ^{137}Cs from the catchment [%] was calculated by dividing the cumulative flux of ^{137}Cs from the catchment L [Bq] by the catchment area S [m^2] and the initial deposition density of ^{137}Cs D [Bq m^{-2}].

Effective environmental half-life

The effective environmental half-life $T_{\text{eff_total}}$ (the period until the concentration of suspended ^{137}Cs is reduced to half of its initial value) from October 2012 to December 2020 was calculated using the results of the suspended ^{137}Cs concentration measurements. In a previous study, Taniguchi *et al.* (2019) [8] reported effective environmental half-lives of 1–4.5 years after the accident (April 2012 to August 2015). In this study, the effective environmental half-life (T_{eff}) was calculated in tree period, $T_{\text{eff_1}}$ for the first period (from October 2012 to March 2016) and $T_{\text{eff_2}}$ for the subsequent period (from March 2016 to December 2020), and $T_{\text{eff_total}}$ for the total period (from October 2012 to December 2020). We then compared the T_{eff} values of suspended ^{137}Cs for each of the three periods.

Catchment characteristics

The catchment characteristics for each observation point were obtained in a manner similar to that described by Taniguchi *et al.* (2019) [8]. Catchment polygons were created using ArcGIS from the coordinates of each observation point and the 10-m digital elevation map (DEM) of Fundamental Geospatial Data by Geospatial Information Authority of Japan (GSI). The catchment area S [km^2] was obtained by calculating the area of the polygon, and the relative altitude was calculated as the difference in elevation between the highest and lowest points in the catchment polygon by averaging the slope values for each grid point calculated from the same DEM over the catchment area. The average slope is the slope value for each grid point calculated from the same DEM and averaged over the catchment. The deposition density D [Bq m^{-2}] was calculated by averaging the value of ^{137}Cs deposition by Kato *et al.* (2019) [18] over the range of catchment polygons created when calculating S . The deposition amount [Bq] was calculated by taking the product of D and S above. The percentage of the catchment area of dams in the watershed was calculated by calculating the catchment area of each of the 10 large dams (Shichigasyuku, Surikamigawa, Miharu, Mano, Oogaki, Yokokawa, Sengosawa, Takashiba, Shitoki, and Takano-kura) that existed in the study area and then calculating the ratio of the sum of the catchment areas of the dams in the watershed to the catchment area S of the observation sites (Table 1).

Results

Change in suspended ^{137}Cs concentration

Figure 2 shows the temporal changes in the concentration of suspended ^{137}Cs from August 2011 to December 2020. In this period, the concentrations of suspended ^{137}Cs ranged from 120 Bq kg^{-1} to $6.33 \times 10^4 \text{ Bq kg}^{-1}$, and with a rapid initial decrease during first year after the accident, and a more gradual decrease thereafter (Fig. 2). The concentration of suspended ^{137}Cs at Iwa in the Abukuma River system in December 2020 was 1.8 % of its initial value 0.33 years after the accident. Similarly, for the Oji and Kit sites, the suspended ^{137}Cs concentrations in December 2020 were 2 % and 2.5 % of the values measured immediately after the accident (0.47 years), respectively. For other sites, the suspended ^{137}Cs concentrations in December 2020 ranged from 5.8 % to 23.5 % of the values measured in October 2012.

The relationship between the suspended ^{137}Cs concentration (Y) and the number of years since the FDNPP accident (t) was approximated using equation $Y = a_1 \times e^{k_1 t} + a_2 \times e^{k_2 t}$ ($p < 0.0001$) for each location. Here, k_1 ranged from 0.68 (Tak) to 19.80 (Kit), with relatively high values of 10 or more at the Mat and Kit sites and relatively low values at the Tak (0.68) and Ona (0.69) sites. Coverage of forest (%) was high at sites Mat and Kit, which are 80.6 % and 55.3 % respectively. At other sites, higher k_1 values tended to indicate relatively high coverage of grassland, bare land, and water. On the other hand, k_2 values ranged from 0.00 (Tak and Ona) to 0.32 (Kit), with k_2 values for nine of the sites, excluding the Tak and Ona sites, ranged from 0.21 (Oji) to 0.32 (Kit), showing no significant differences among the sites (standard deviation: 0.05) (Table 1). Lower k_2 values tended to indicate relatively high coverage of urban areas.

Effective environmental half-lives (T_{eff}) were calculated based on temporal changes in suspended ^{137}Cs concentrations (Table 1). $T_{\text{eff_total}}$ for the period from October 2012 to December 2020, ranged from 2.18 to 5.45 years; $T_{\text{eff_1}}$ (1.7–5 years after the accident) for the period 2012/10–2016/4, ranged from 1.37 to 3.49 years; $T_{\text{eff_2}}$ (5–10 years after the accident) for the period 2016/4–2020/12 was 2.33–11.51 years. The effective environmental half-life, $T_{\text{eff_1#}}$ (1–4.5 years after the accident) was also reported 1.45–11.36 years by Taniguchi et al. (2019) [8]. However, in samples with very small amounts collected, the ^{137}Cs concentration was close to the detection limit, which may have caused a difference between the measured and actual concentrations. This may have caused errors in the calculation of the T_{eff} values. For example, $T_{\text{eff_1#}}$ at Oda was 11.36 years, which was one order of magnitude

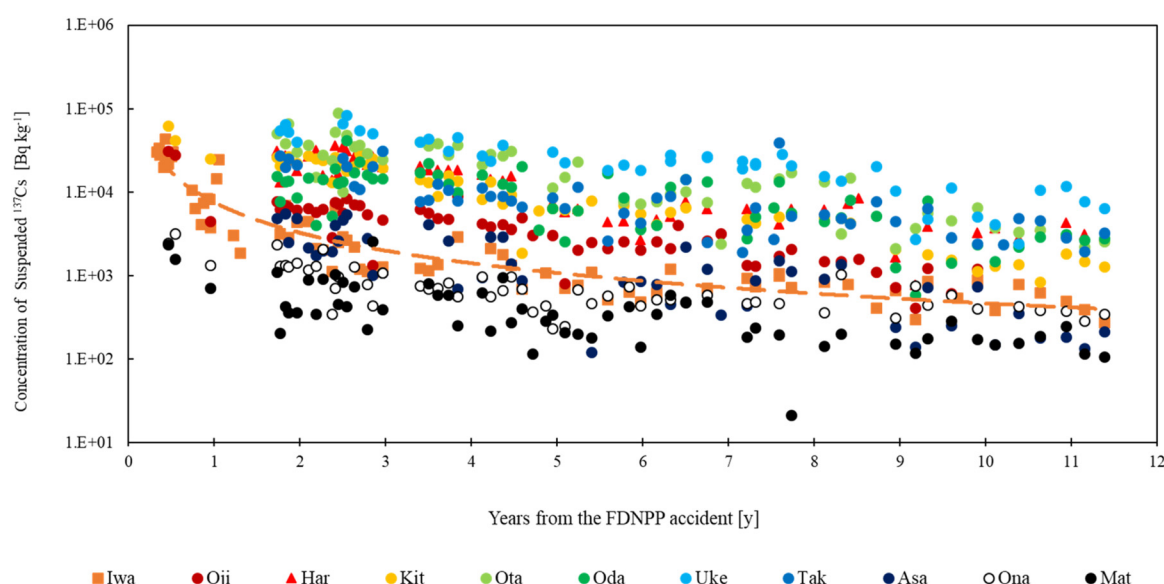


Fig. 2: Time series of the radioactivity concentrations of suspended ^{137}Cs .

higher than that at the other sites; therefore, the sample was re-measured (suspended ^{137}Cs concentration 5.08 years after the accident: 4000 Bq/kg) and recalculated, resulting in an updated $T_{\text{eff_1}}$ of 3.49 years for Oda. The arithmetic mean (median) of $T_{\text{eff_total}}$, $T_{\text{eff_1}}$, $T_{\text{eff_1#}}$, and $T_{\text{eff_2}}$ for the 11 sites were 3.04 ± 0.64 (2.95) years, 3.46 ± 1.76 (2.39) years, 3.46 ± 1.76 (2.77) years, and 4.95 ± 2.49 (4.47) years, respectively. The T_{eff} values were found to increase 10 years after the accident (Table 1).

Monthly flux of suspended ^{137}Cs

The monthly suspended ^{137}Cs fluxes from August 2011 to December 2020 ranged from 1.46×10^6 Bq to 3.41×10^{12} Bq, with the highest monthly flux measured at Iwa in September 2011 and the lowest flux at Asa in March 2013 (Fig. 3). The catchment area of the Abukuma River at the Iwa site is the largest among the nine rivers (5313.2 km^2 , Table 1), whereas that of the Asami River at the Asa site is the smallest (25.8 km^2 , Table 1). The difference in ^{137}Cs fluxes could be attributed to the difference in the catchment areas, which span two orders of magnitude. Several peaks of monthly fluxes of suspended ^{137}Cs were observed in September 2015 (Iwa, Har, Tak, Oda, Ota, etc.), August 2016 (Uke, Asa, Har, etc.), October 2017 (Uke, Iwa, Asa, Oda, etc.), and October 2019 (Iwa, Uke, Asa, etc.) (Fig. 3). At all sites, the monthly flux of suspended ^{137}Cs decreased over time, although a few peaks were observed during the monitoring period (Fig. 3). In particular, at the Iwa site, the monthly flux of suspended ^{137}Cs decreased exponentially with time according to the follow equation: ($X = \text{year}$) ($y = 2.0 \times 10^{11} e^{-0.024x}$, $R^2 = 0.4165$).

The fluxes of ^{137}Cs depend on the situation of water flow. Since the concentration of suspended ^{137}Cs has been reduced to about one-tenth over the past decade, it is expected that the actual ^{137}Cs flux reduction was 76–98 % if there is an equivalent water flow. Whereas the physical ^{137}Cs flux reduction was 16.6 % for radiative modification, the actual ^{137}Cs flux reduction is far more important.

Cumulative fluxes of suspended ^{137}Cs

The highest cumulative flux of suspended ^{137}Cs from October 2012 to December 2020 was observed in Iwa (6.48×10^{12} Bq), followed by Uke (4.61×10^{12} Bq), Har (2.81×10^{12} Bq) and Tak (1.92×10^{12} Bq) (Fig. 4). The same trend was observed for the initial deposition of ^{137}Cs (Bq) in each catchment area, with Iwa (4.70×10^{14} Bq) exhibiting the highest deposition, followed by Uke (3.92×10^{14} Bq), Har (1.93×10^{14} Bq), and Tak (1.91×10^{14} Bq). This suggests that

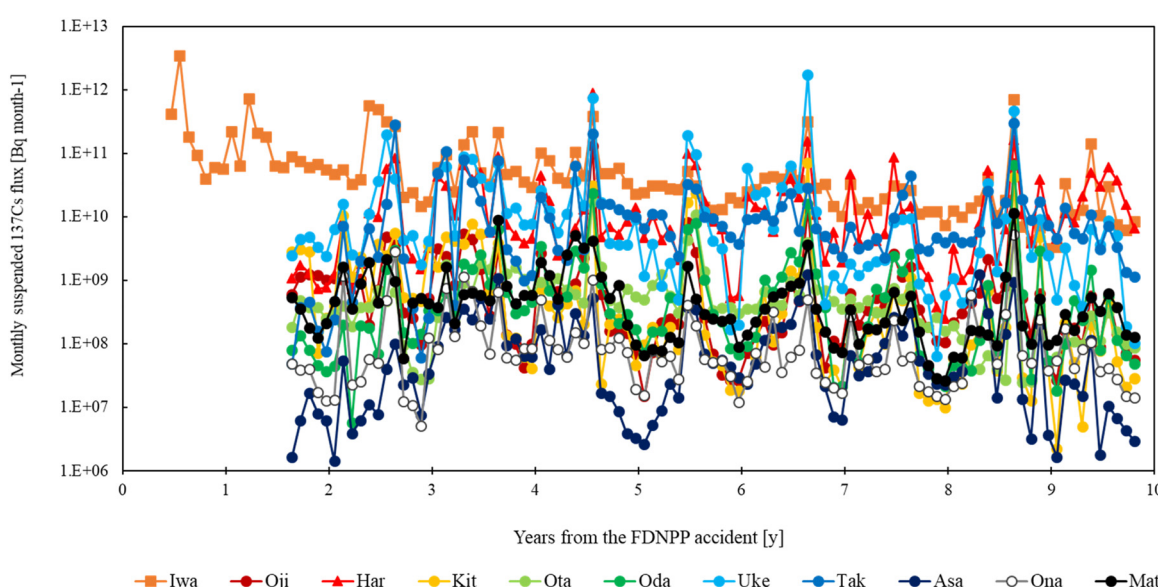


Fig. 3: Monthly suspended ^{137}Cs flux in each site. The data of [Iwa] is shown from 0.33 years after the accident; and the others were measured from 1.7 years after the accident.

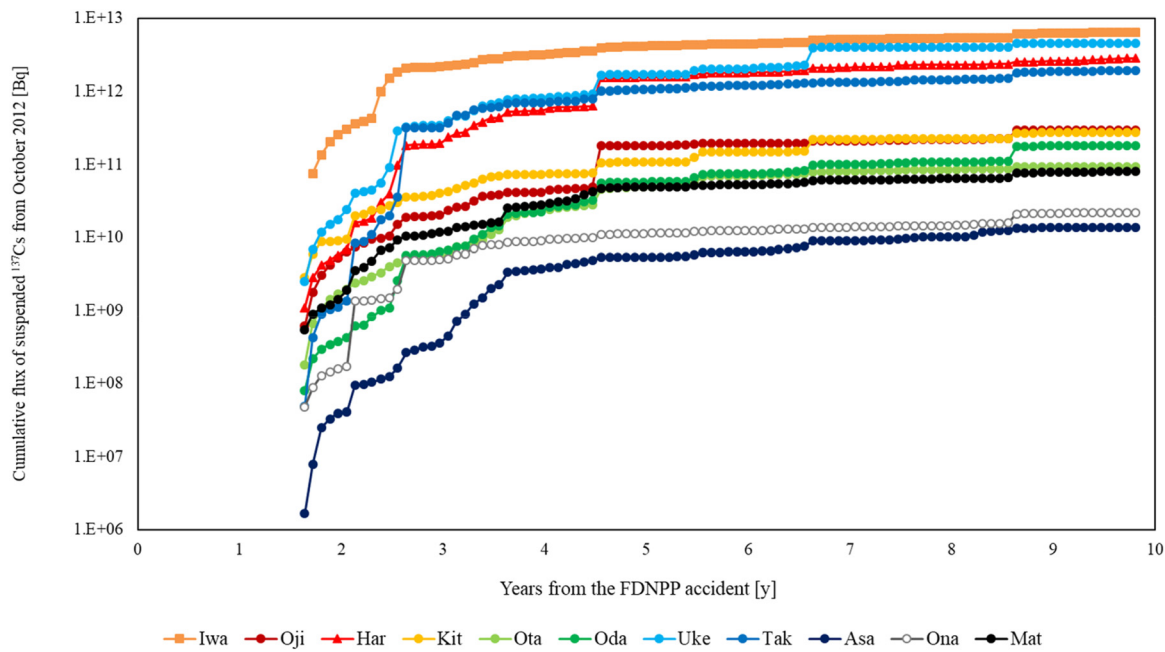


Fig. 4: Cumulative flux of suspended ^{137}Cs in the rivers in Fukushima area since October 2012.

one of the reasons for the high cumulative flux of suspended ^{137}Cs in 2012–2020 was the high amount of initial ^{137}Cs deposition in the catchment area. Asa, which has the smallest catchment area, had the lowest cumulative flux of suspended ^{137}Cs at 1.38×10^{10} Bq, which was two orders of magnitude lower than that of Iwa (Fig. 4). The timing and amount of change in the integrated amount of suspended ^{137}Cs flux varied significantly from site to site. The total flux of suspended ^{137}Cs at the 11 sites was 17 TBq (Fig. 4).

The cumulative amount of suspended ^{137}Cs flux at Iwa increased by approximately two orders of magnitude from 10^{10} Bq to 10^{12} Bq from October 2012 to July 2013, and then remained in the order of 10^{12} Bq. The flux at Uke increased by two orders of magnitude from 10^9 Bq to 10^{11} Bq from October 2012 to September 2013, reaching 10^{12} Bq by September 2015, and then remaining at the 10^{12} Bq order. Har showed a two orders of magnitude increase from 10^9 Bq to 10^{11} Bq from October 2012 to October 2013, followed by a gradual increase from 10^{11} Bq in August 2015, to 10^{12} Bq by September 2015. Tak increased by approximately four orders of magnitude from 10^7 Bq to 10^{11} Bq until October 2013, and then increased moderately to 10^{12} Bq. Ona gradually increased to 10^9 Bq in April 2013 and then to 10^{10} Bq in October 2015. The Kit site cumulative flux reached 10^{10} Bq by April 2013, increasing by one order of magnitude thereafter, and remaining at 10^{11} Bq since September 2015. Oji increased from 10^8 Bq to 10^{10} Bq by August 2013, then slowly increased to 10^{10} Bq, and remained at 10^{11} Bq from September 2015. Mat increased from 10^8 Bq to 10^{10} Bq in October 2013, and has remained at 10^{10} Bq since then. Ota increased by approximately one order of magnitude each in October 2012 and August 2014, followed by a gradual increase to 10^{10} Bq. Oda increased from 10^8 Bq to 10^{10} Bq in July 2014, and steadily increased to increase to 10^{11} Bq by November 2017. Asa increased from 10^6 Bq to 10^9 Bq in June 2014, followed by a gradual increase to 10^{10} Bq.

Cumulative loss of suspended ^{137}Cs to initial deposition

Cumulative loss of ^{137}Cs from the catchment to initial deposition (hereinafter referred to as “Cumulative loss of ^{137}Cs ”) at each site ranged from 0.1 to 1.7 % from October 2012 to December 2020 (Fig. 5). Cumulative loss of ^{137}Cs was highest in Har (1.7 %), followed by Kit, Uke, Iwa, Tak, Ona, Oji, Ota, Mat, Asa, with the lowest in Ota (0.12 %). The Niida River, located in Har, had the second highest normalized discharge ($1.40 \times 10^9 \text{ kg km}^{-2} \text{ year}^{-1}$, Table 1), while the Ota River, with Ota, had the lowest normalized discharge ($4.17 \times 10^8 \text{ kg km}^{-2} \text{ year}^{-1}$, Table 1).

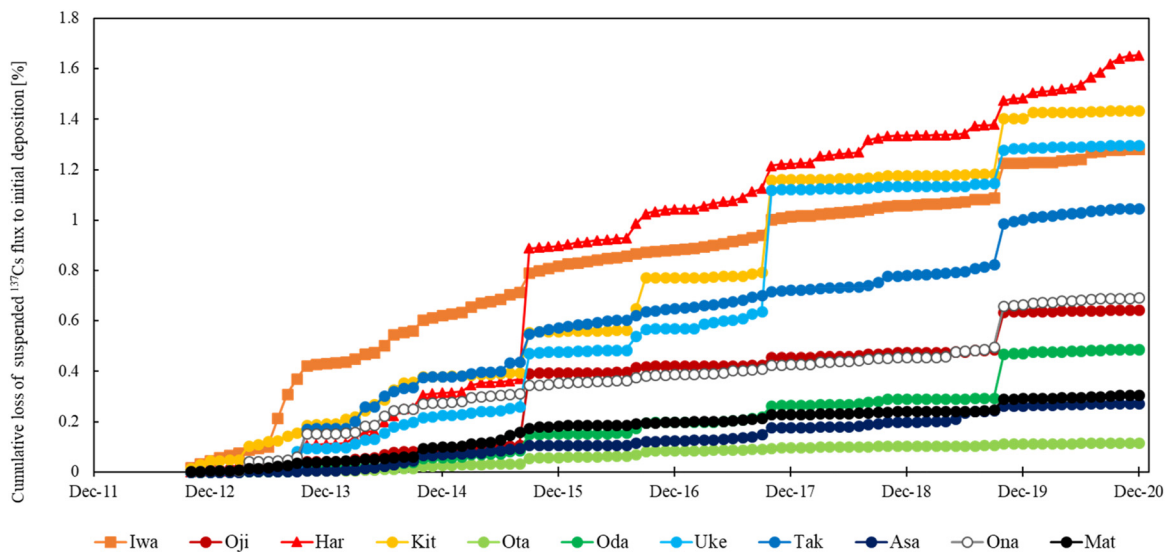


Fig. 5: Cumulative loss of suspended ^{137}Cs flux from the catchment to initial deposition [%]. Monthly flux was accumulated from October 2012 and then divided by the initial deposition.

Before August 2015, the cumulative loss of ^{137}Cs from the catchment in Iwa was almost highest (0.08 %), while at Har, the cumulative loss of ^{137}Cs increased by approximately 0.6 %, from 0.3 % to 0.9 %, following Typhoon Etau in September 2015 and subsequently was the highest among the 11 sites. The cumulative loss of ^{137}Cs at the Har site increased slightly in October 2017 and again in October 2019, with a peak in the suspended ^{137}Cs flux during the same period (Fig. 3). The monthly fluxes of suspended ^{137}Cs including the three runoff periods (September 2015, October 2017, and October 2019) at the Har site, corresponded to 89 %, 50 %, and 71 % of the annual flux, respectively. The monthly suspended ^{137}Cs flux to the initial deposition in September 2015, October 2017, and October 2019 were 0.52 %, 0.09 %, and 0.14 %, respectively. An increased cumulative loss of ^{137}Cs was also observed at sites Uke, Kit, Oji, and Oda in September 2015, and at sites Kit and Uke in October 2017, and at sites Kit, Uke, Iwa, Tak, Oji and Ona in October 2019.

Thus, the cumulative loss of ^{137}Cs increased at several sites in accordance with the timing of the large-scale runoff caused by Typhoon No. 18 in September 2015, Typhoon No. 21 in October 2017, and Typhoon No. 19 in October 2019 (East Japan Typhoon in 2019). However, the cumulative loss of ^{137}Cs differed at each site. The timing of the increase in the cumulative loss of ^{137}Cs at each site can be explained, to some extent, by the change in the normalized discharge of each river (Fig. 6). The cumulative loss of ^{137}Cs at the Kit site temporarily exceeded the value at the Iwa site in June 2013, but the normalized discharge of Kit was higher than that of Iwa during the same period. In 2015, when the rankings switched frequently, Kit had the highest normalized discharge, followed by Har, Uke, Oji, and Tak, with higher normalized discharges of 28.4, 14.1, 12, 9.2, and 5.8 times the normal discharge at each site, respectively. However, in September 2015, the cumulative loss of ^{137}Cs at the Har site was the largest, with the fourth highest normalized discharge, suggesting that other factors should be further investigated. Subsequently, the cumulative loss of ^{137}Cs at the Iwa site continued in second place until September 2017 and was surpassed by the Kit and Uke sites during Typhoon [Lan] in 2017. Since 2017, the order locations have been fixed at the five sites of Har, Kit, Uke, Iwa, and Tak, and this trend has not changed, even after a large typhoon in 2019.

The normalized discharge of sites where the cumulative loss of ^{137}Cs was high also showed a similar trend during the two runoff periods in 2017 and 2019. In 2020, the cumulative loss of ^{137}Cs of each river remained almost unchanged. However, an increase is observed at the Har site. This is consistent with the relatively high annual normalized river discharge in 2020 compared with other years (Fig. 6) and may be due to the relatively high precipitation in 2020 (Ministry of Land, Infrastructure, Transport and Tourism, Japan Meteorological Agency HPP <https://www.data.jma.go.jp/stats/etrn/index.php>).

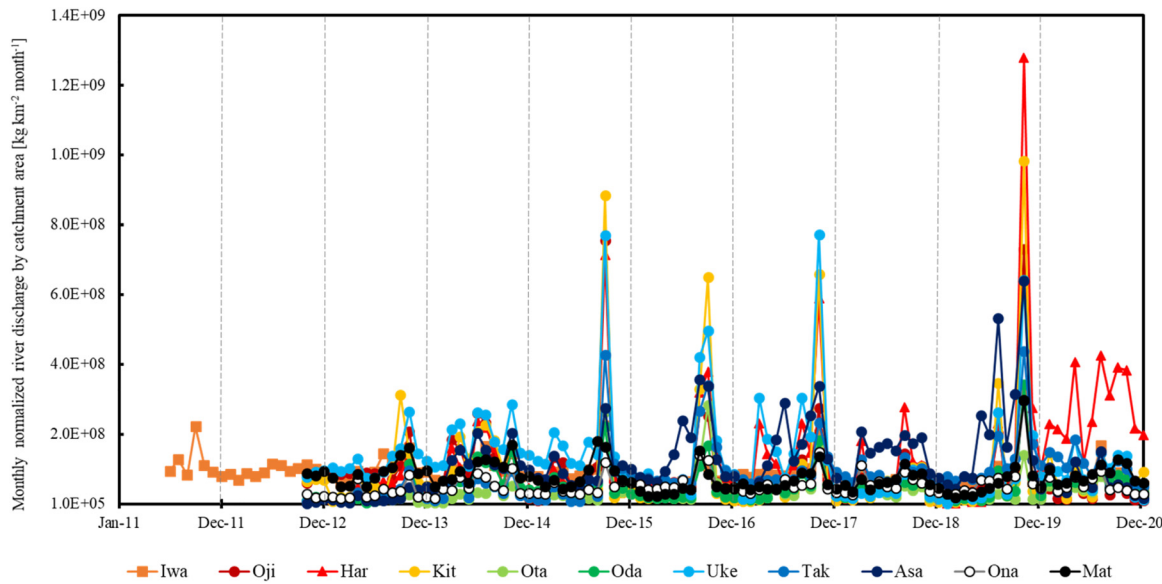


Fig. 6: Monthly normalized river discharge by catchment area. The data is calculated by the measured water level value and the $h\text{-}Q$ curve and then divided by the area of the catchment.

The physical decay of ^{137}Cs between October 2012 and December 2020 can be calculated 16.6 % of the initial ^{137}Cs deposition since the half-life of 30 years. Relative to the cumulative loss of suspended ^{137}Cs through rivers in this decade, which was accounted 0.1–1.7 % of the initial ^{137}Cs deposition. For the reduction of ^{137}Cs deposited in terrestrial by FDNPP accident, physical decay has contributed more than the cumulative loss of ^{137}Cs during the decade.

Discussion

Suspended ^{137}Cs fluxes through rivers

In this study, the total amount of suspended ^{137}Cs released from coastal rivers into the ocean over the period October 2012 to December 2020 was 17 TBq, which represents 0.6 % of the 2.7 PBq of ^{137}Cs deposited on land in the Fukushima Prefecture. Using a mass balance approach, Aoyama et al. (2020) [19] estimated that the amount of ^{137}Cs transferred from land to the ocean via rivers around the FDNPP was 10–12 TBq/yr. Sakuma et al. (2019) [20] used a tank model to estimate the flux of 14 rivers in the Fukushima coastal area during the first six months after the accident to be 29 TBq, to which the flux in the Abukuma River, the largest river in Fukushima Prefecture, contributed 18 TBq. Taniguchi et al. (2019) [8] found that the actual flux of suspended ^{137}Cs in the Abukuma River (Iwa site) was 4.2 TBq in 2011 (August–December) and was 1.9 TBq in 2012. In this study, the amount of suspended ^{137}Cs was estimated to be 6.48 TBq in the Abukuma River (Iwa site) for the period 2012–2020. The total amount of ^{137}Cs from June 2011 to August 2015 was estimated to be 12 TBq (96.5 % of which was suspended) [16], with the contribution of ^{137}Cs outflow in 2011 being particularly significant.

In addition, in the Abukuma River, the largest river in Fukushima Prefecture, the amount of suspended ^{137}Cs was estimated to be 5.8 TBq from June 2011 to September 2012 (calculated according to Fig. 3). Previous observations and studies have reported that, from June 2013 to December 2016, the estimated amount of ^{137}Cs entering the ocean was 26 GBq in the Mano River and 19 GBq in the Hiso River (an upstream tributary of the Nitta River) [21]. Correspondingly, from 2013 to 2016, the estimated values in the lowest reaches of the Mano River (Oji site) and the Nitta River were 185 GBq and 779 GBq, respectively. For the three times of ^{137}Cs transported during runoff

periods in the Nitta River from 2019 to 2020, the ^{137}Cs flux ranged from 0.33 to 19 GBq (including 0.23–18.8 GBq in suspended form) [9], resulting in monthly suspended ^{137}Cs fluxes including the three outfalls of 9.27–64.3 GBq respectively.

Factors contributing to the decrease of suspended ^{137}Cs flux

The decrease in the amount of suspended ^{137}Cs transported was inferred from variations in the suspended ^{137}Cs concentration, suspended ^{137}Cs flux, river discharge, and SS fluxes. At site Iwa, the monthly suspended ^{137}Cs flux decreased, and the variability in annual river normalized discharge was smaller than that at other sites during the period (2012–2020) of this study (Fig. 7). In addition, there was no correlation between SS flux and the number of months since the FDNPP accident (Supplementary material Table 4). Therefore, the low suspended ^{137}Cs flux may have been due to a decrease in suspended ^{137}Cs concentrations over time. This is similar to the results of a previous study conducted on the Abukuma River [10].

Uke had the largest initial deposition of ^{137}Cs (Table 1), and the change in monthly suspended ^{137}Cs flux also showed a decrease trend from 2012 to 2020 ($y = 3.0 \times 10^{10} e^{-0.262x}$, $R^2 = 0.1085$). The pattern of change in annual normalized discharge in the river increased until 2017, followed by a decreasing trend. During the period of increased annual normalized discharge until 2017, suspended ^{137}Cs fluxes continued to decrease. Temporal changes in the SS fluxes were small, as at the Iwa site. Based on the above, the rapid decrease in suspended ^{137}Cs concentrations from the time of the FDNPP accident to the early years (2017) was considered the main contributor to the decrease in flux. The decrease in both the suspended ^{137}Cs concentrations and river-normalized discharge from 2017 to 2020 may have contributed to the decrease in the suspended ^{137}Cs flux.

Considering the entire 2012–2020 period, it appears that different factors contributed to the decrease in suspended ^{137}Cs flux at the Har and Tak sites compared to the other sites. The main reason for this is that the suspended ^{137}Cs monthly flux for the first two years (2012–2014) increased and fluctuated. However, after 2014, suspended ^{137}Cs fluxes began to decrease. Annual normalized discharge for the river at site Tak was low for the first two years ($3.42\text{--}4.47 \times 10^8 \text{ kg km}^{-2} \text{ year}^{-1}$), then began to increase in 2014 and increased by an order of

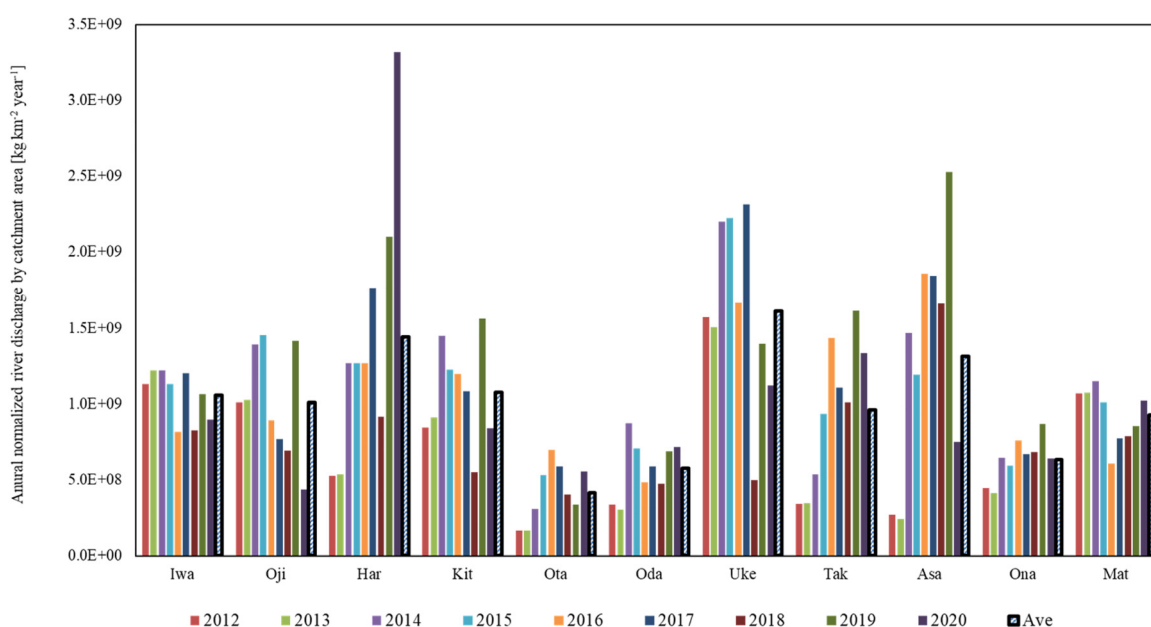


Fig. 7: Annual normalized river discharge by catchment area in rivers from 2012 to 2020. Averages were calculated using data from 2012 to 2020.

magnitude after 2015, reaching $0.94\text{--}1.61 \times 10^9 \text{ kg km}^{-2} \text{ year}^{-1}$ (Supplementary material Table 3). In other words, suspended ^{137}Cs concentrations decreased, but the annual normalized discharge of the river doubled, resulting in no decrease in the suspended ^{137}Cs flux during the first two years at the Tak site.

A further special aspect of the Har site is that throughout the entire period from 2012 to 2020, the annual river-normalized discharge has shown an increasing trend (Fig. 7) due to increased rainfall. However, after 2014, the suspended ^{137}Cs flux began to decrease. In other words, at the Har site, the increased river-normalized discharge and decreased suspended ^{137}Cs concentrations mutually counteracted each other. However, after 2014, the effect of the decrease in concentrations seems to have exceeded the effect of the increase in river-normalized discharge. This countervailing effect was also evident in the large outflows: the monthly river-normalized discharges for typhoons in September 2015 (Etau), October 2017 (Lan), and October 2019 (Hagibis) were $7.13 \times 10^8 \text{ kg km}^{-2}$ and $5.89 \times 10^8 \text{ kg km}^{-2}$ and $1.28 \times 10^9 \text{ kg km}^{-2}$ (Supplementary material Table 3), and the corresponding monthly fluxes of suspended ^{137}Cs were $8.91 \times 10^{11} \text{ Bq}$, $1.55 \times 10^{11} \text{ Bq}$ and $1.63 \times 10^{11} \text{ Bq}$ (Supplementary material Table 5). On the other hand, the monthly fluxes of SS were $1.18 \times 10^8 \text{ kg}$, $2.44 \times 10^7 \text{ kg}$, and $9.73 \times 10^7 \text{ kg}$, respectively (Supplementary material Table 4). The SS fluxes during Typhoon Hagibis (2019) were estimated to be four times higher than those during Typhoon Lan (2017), while the monthly fluxes of suspended ^{137}Cs showed almost the same values. The reason for this similarity was that the concentration of suspended ^{137}Cs decreased over time. In addition, although the river-normalized discharge in Typhoon 2015 (Etau) and Typhoon 2017 (Lan) were of similar magnitude (the value in 2015 was 1.2 times larger) at this site, the amount of SS flux was nearly five-fold larger in 2015 (Etau), and the suspended ^{137}Cs flux was also about 6 times higher in 2015. This indicates that the SS flux during large runoff events is a factor in suspended ^{137}Cs transport.

The monthly SS flux was 158 times higher during Typhoon Etau (2015) than the average monthly flux of 2015, reaching a highest peak at the Har site (Supplementary material Table 4). The reason for the large SS flux was thought to be the decontamination activities conducted from August 2012 to December 2016 in the upper reaches of the Nitta River, where the Har site is located. These activities removed the land surface layers of PFU (paddy fields, fields, and urban) area and increased soil particle runoff from the land surface during and immediately after the decontamination period. An evaluation of the impact of decontamination works from 2013 to 2018 in an existing study in Har reported that the soil erosion rate in 2016 reached 216 % compared to 2013 before decontamination [22]. This is consistent with the SS fluxes considered in this study. However, along with the decontamination work, the decrease in the suspended ^{137}Cs concentration in the river was not significantly different from that in other areas where decontamination was not performed (Fig. 2). This may be due to the large coverage of forest and grassland (>90 % [8]; Table 1) in the catchment at the Har site, which diluted the decontamination effect in PFU area. The monthly SS fluxes after 2016 increased in a stepwise manner compared with the data before 2016, showing an increasing trend. The suspended ^{137}Cs flux was caused by the synergistic effects of lower suspended ^{137}Cs concentrations, increased river-normalized discharge, and increased SS fluxes at the Har site.

The results of this study indicate that the decrease in suspended ^{137}Cs concentration is the main factor influencing the decrease in the flux of suspended ^{137}Cs and that river-normalized discharge also contributes to the decrease. Although the large-scale runoff caused a large amount of suspended ^{137}Cs transport, the suspended ^{137}Cs concentrations continued to decrease and returned to Pre-Storm Level soon after the runoff (Figs. 3 and 6); thus, there is little concern about the impact on the livelihoods of people downstream. Studies on the origin of SS during runoff and normal periods have indicated that suspended ^{137}Cs concentration during runoff may further decrease due to the dilution of riverbed soil and river sediment, which have lower ^{137}Cs concentrations [23].

Factors affecting the cumulative loss of suspended ^{137}Cs to initial deposition [%]

The possible factors affecting the cumulative loss of suspended ^{137}Cs fluxes to initial deposition include (1) the coverage of the dam in the catchment area, (2) the effect of river discharge, and (3) the effect of SS fluxes. First, regarding the coverage of dams in the catchment area, the cumulative loss of suspended ^{137}Cs to the initial deposition varied significantly among rivers (Fig. 5). Both Ota and Mat sites, where the loss was low, had dams located upstream. The coverage of dams in each catchment area was 90 % and 89.3 % respectively (Table 1). To

examine the effect of dam coverage in the catchment area on the cumulative loss of suspended ^{137}Cs from the catchment, this study compared the site with dams in the upper reaches of the river and found that the cumulative loss of suspended ^{137}Cs from the catchment was lower with higher dam coverage. A clear negative correlation ($y = -0.016x + 1.770, R^2 = 0.742$) was observed between the two variables (Fig. 9a). The cumulative loss of suspended ^{137}Cs from the catchment was lower when the dam coverage was higher, suggesting that dams play a buffering role in the movement of suspended ^{137}Cs .

The water body of a dam lake, from the river inflow area to the dam site, can be divided into three zones along the downstream direction: the riverine zone of well-mixed flow, the transition zone of suspended sediment deposition, and the lacustrine zone of water mass fractionation. It is generally thought that the greater the annual discharge in a larger catchment area and the greater the amount of SS where the dam lake with greater the discharge [24]. Dams in the radiologically contaminated areas of Fukushima Prefecture are used for irrigation, industry, drinking water, etc. and are managed to provide sufficient sediment storage capacity for the inflow sediment to be deposited and to capture less turbid water from the surface or upper layers. The Matsugafusa Dam, located on the Uda River flowing through northern Fukushima Prefecture, has been shown to be effective in reducing SS-associated ^{137}Cs transport from the upstream dam catchment to the downstream area by over 85 % [25]. The ability of dams to accumulate ^{137}Cs associated with inflow sediments plays an important role in preventing the spread of ^{137}Cs from heavily contaminated upstream areas to slightly contaminated downstream agricultural and urban areas. Several studies conducted after the Chernobyl accident qualitatively evaluated this storage effect by comparing the concentrations of SS and SS-related ^{137}Cs in the inflow and outflow of dams in contaminated areas [26, 27]. The results of this study (Fig. 9a) showed that the coverage of dams in the catchment area was an effective factor influencing the long-term (2012–2020) cumulative suspended ^{137}Cs fluxes.

In addition, the correlation between the values of T_{eff} of suspended ^{137}Cs and the coverage of dams also reflected the storage effect of dams on SS (Fig. 9b). There was a strong positive correlation ($y = 0.056x + 0.235, R^2 = 0.509$) between $T_{\text{eff},1}$, calculated with data for the first five years after the accident as the period, and the coverage of the dam catchment area. Because the concentration changes more slowly with longer T_{eff} values, it is considered that more SS containing suspended ^{137}Cs is stored in areas with a larger dam coverage. Previous studies have also shown that the accumulation of suspended ^{137}Cs by dams and subsequent dissolution increased the concentrations of dissolved ^{137}Cs in the dams [25, 28]. Although there is a possibility of an increase in the concentration of dissolved form, the amount is considered to be small [29]. However, because of the rapid decrease in suspended ^{137}Cs concentrations in the river, no correlation was found between dam coverage and $T_{\text{eff},2}$ as a period between 5 and 10 years after the accident. As a result, the relationship between the dam coverage and $T_{\text{eff},\text{total}}$ was weaker than that with $T_{\text{eff},1}$. Activities, such as dam drainage and storage, also play a role in regulating river discharge. The combination of the effects of SS accumulation and water flow regulation may have resulted in the correlation between the cumulative loss of ^{137}Cs from the catchment and the coverage of dams in the catchment.

Next, regarding to the effect of river discharge, a positive correlation ($y = 9 \times 10^{-10}x - 0.0519, R^2 = 0.378$) was observed between the mean annual river normalized discharge and the cumulative loss of suspended ^{137}Cs from the catchment for all sites (Fig. 8c). The normalized discharge for each catchment, defined as “monthly normalized discharge”, represented seasonal variations clearly (Fig. 6). To determine the overall status of the catchment over the years (2012–2020), the annual normalized discharge and 9-year averages are shown in Fig. 7. In the Fukushima Prefecture, the annual normalized discharge of the “Abukuma” River, a major river with a largest catchment area, and the “Same” River, which affected by dams, were relatively stable. However, rivers with smaller catchment areas and no dams in their upper reaches (e.g., Ukedo River and Niida River) were more sensitive to rainfall and prone to large fluctuations in annual normalized discharges. We also showed that the forest coverage in the catchment area affected the annual normalized discharge (Fig. 8b). Suspended ^{137}Cs in river water is absorbed by soil particles in the catchment, transported from the ground surface to the river via precipitation, and then transported downstream. It has been reported that suspended ^{137}Cs flux is related to the amount and intensity of precipitation [9]. In recent years, annual rainfall has been increasing, and annual normalized discharges have also increased (Fig. 7). Therefore, a higher annual normalized discharge could lead to a greater amount of suspended ^{137}Cs transported from the upper reaches of the river. In rivers where the annual

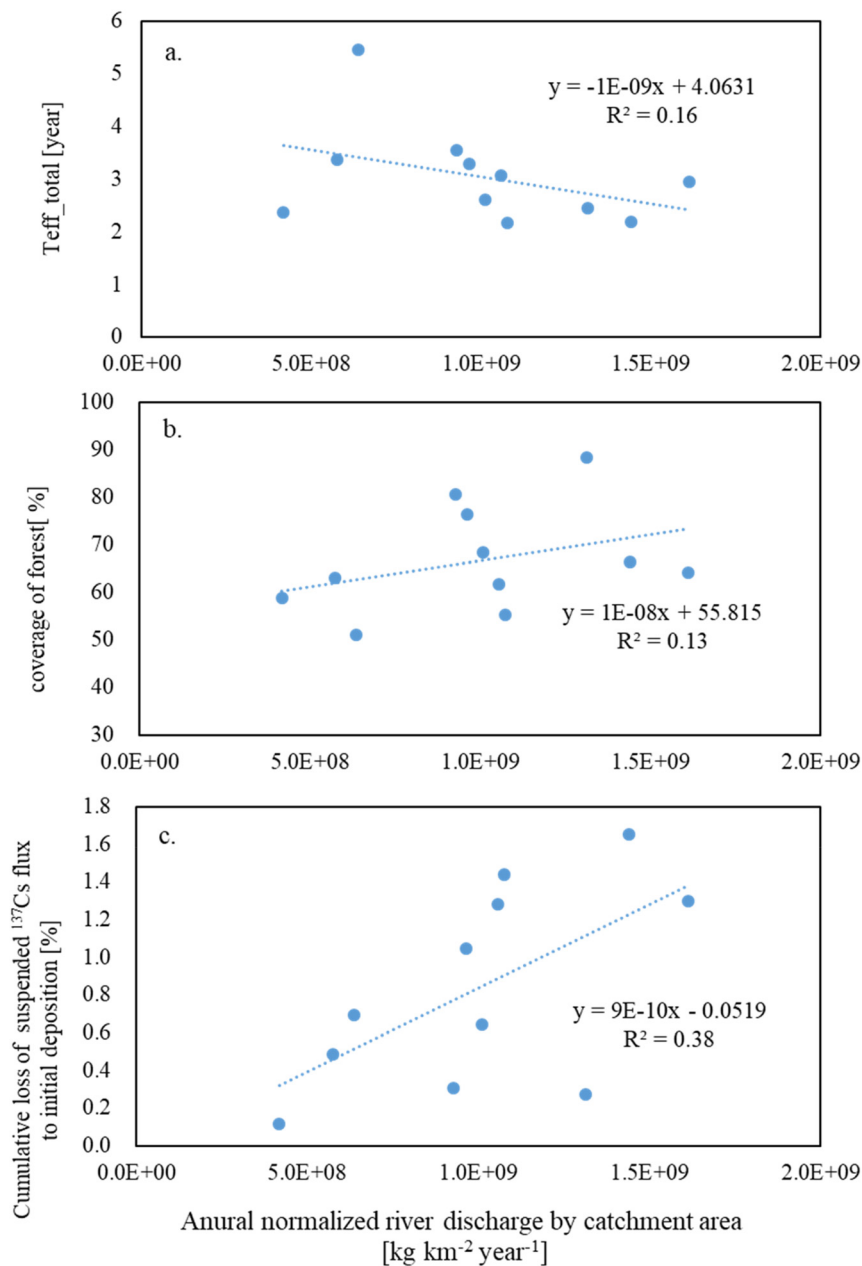


Fig. 8: Relationship between the average annual water flow per unit catchment area and (a) $T_{\text{eff_total}}$: the effective ecological half-lives for the total period, (b) coverage of forest [%], (c) cumulative loss of suspended ^{137}Cs flux to initial deposition [%]. Averages were calculated using data from 2012 to 2020.

normalized discharge is small, the variation in the cumulative loss of ^{137}Cs from the catchment is also large because the normalized discharge tends to change in accordance with changes in precipitation. The variation in the cumulative loss of ^{137}Cs from the catchment was particularly large at sites with a high initial deposition of ^{137}Cs at the Uke and Har sites. The effective environmental half-life, $T_{\text{eff_total}}$, tended to be shorter at sites with higher average annual normalized discharge values (Fig. 8a), indicating a faster decrease in suspended ^{137}Cs concentrations.

Regarding to the effect of SS flux, the SS monthly fluxes showed the most significant increasing trends at the Har ($R^2 = 0.31$) and Tak sites ($R^2 = 0.28$) (Supplementary material Table 4). These two sites were characterized by an

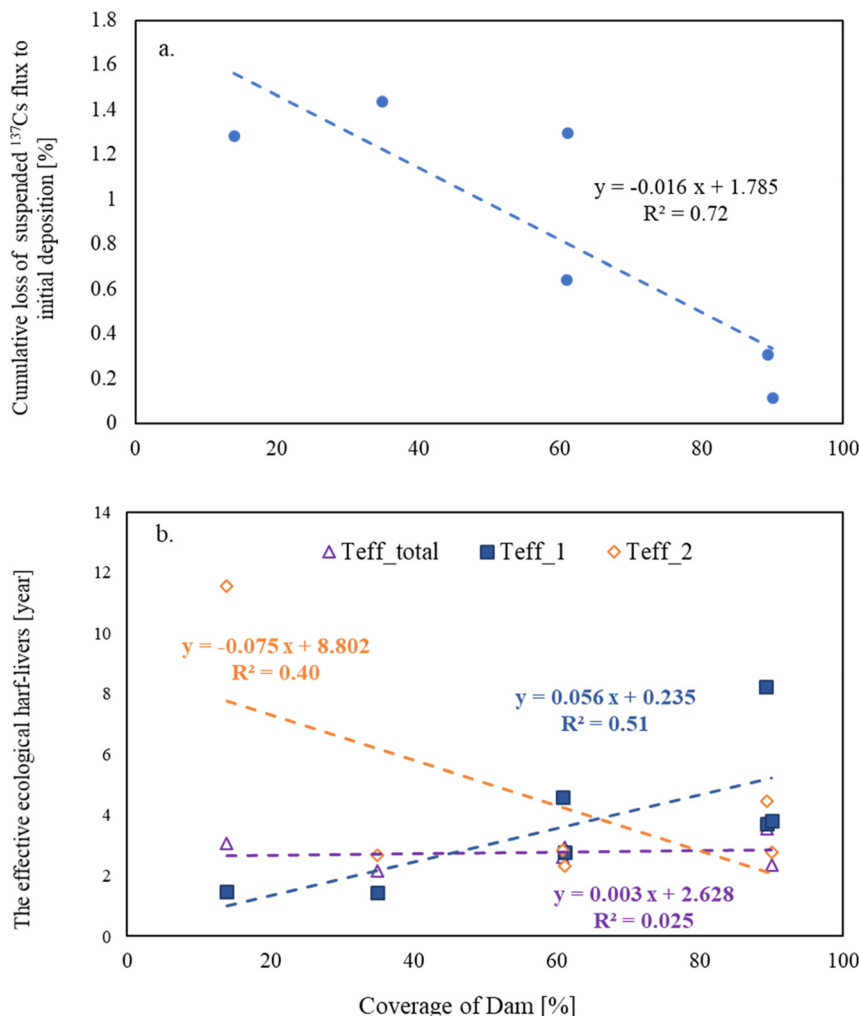


Fig. 9: Relationship between the combined coverage of Dam [%] and (a) cumulative loss of suspended ^{137}Cs flux to initial deposition [%], (b) the effective ecological half-lives [year]. $T_{\text{eff_total}}$, $T_{\text{eff_1}}$ and $T_{\text{eff_2}}$ values for each monitoring site are shown in Table 1.

increase in the annual normalized discharge. Six stations, including Mat, Ota, Oda, and Asa, showed increasing trends in SS flux (Supplementary material Table 4). Four of these six stations did not have dams upstream (Table 1), and the increase in SS flux was considered to be influenced by reduced storage interception by the dams. Therefore, the increase in SS fluxes at these four sites may have been due to increased human activity in the catchment since the nuclear accident. In contrast, no increasing trend in monthly SS flux was observed at stations Iwa, Oji, Ona, Kit, and Uke. Four of these five sites had dams in their upper reaches, and the coverage of dams in catchment ranged from 13.9 to 61.1 %. Ona site, the only one of these five sites without a dam upstream, was not designated as an evacuation zone, and it is likely that no change in human activity was observed.

Therefore, the SS is likely to be affected by river discharge and catchment characteristics (presence or absence of dams in the upstream area, average topographic gradient, etc.). In addition, although the evacuation order immediately after the accident reduced the impact of human activities on vegetation and suppressed the discharge of SS during the evacuation period, the increase in human activity with the gradual lifting of the evacuation order may have contributed to the increasing SS trend.

In this study, we conducted a long-term analysis of the decrease in ^{137}Cs concentration and flux from rivers to the ocean and the associated factors. Future studies on SS fluxes will need to consider many influencing factors, and SS fluxes normalized by each influencing factor will need to be considered.

Conclusions

In this study, we summarized data on the transport of suspended ^{137}Cs from October 2012 to December 2020 at 11 sites in nine rivers affected by the Fukushima Daiichi Nuclear Power Plant accident. The concentration of suspended ^{137}Cs in the rivers decreased to 1/10–1/100 of the initial concentration after the accident. In addition to the concentration of suspended ^{137}Cs , river discharge and SS flux were calculated to determine the amount of suspended ^{137}Cs transferred to the ocean. As a result, the suspended ^{137}Cs flux through the river to the ocean from October 2012 to December 2020 was calculated to be 17 TBq. The coverage of the dam in the catchment at the observation sites influenced the cumulative loss of suspended ^{137}Cs from the catchment, and the suspended ^{137}Cs flux to the ocean was relatively large during large-scale runoff events, such as typhoons.

We found that SS fluxes increased in several catchments. This may be related to the lifting of the evacuation order and an increase in human activities. Furthermore, runoff from forested areas, which account for 71 % of the watershed area in the Fukushima Prefecture, is also thought to contribute to the transport of suspended ^{137}Cs . In addition, it was assumed that long-term runoff occurred, although its amount was small. Further studies are required to determine the flux of ^{137}Cs in the future.

Acknowledgments: This work was supported by ERAN F-21-02, F-22-01, and P-23-02. We would like to thank the staff of the Fukushima Prefectural Centre for Environmental Creation and Mr. Yoshita H., Mr. Fujita K., Mr. Ito H., and Mr. Miyakawa K. for their assistance with the collection and analysis of river water samples.

Research ethics: Not applicable.

Author contributions: S. F. wrote the manuscript. K. N. and Y. T. performed sample collection and experiential operations as well as data verification. M. F. and H. A. participated in the discussion and text modifications. K. T. performed various calculations and statistical analysis. Y. O., who is the host researcher of the research funding, reviewed the first draft of the paper and served as the corresponding author. The authors have accepted responsibility for the entire content of this manuscript and approved its submission.

Competing interests: The authors state no conflict of interest.

Research funding: This work was partially supported by ERAN F-21-02, F-22-01, and P-23-02.

Data availability: The raw data can be obtained on request from the corresponding author.

References

- [1] G. Katata, M. Chino, T. Kobayashi, H. Terada, M. Ota, H. Nagai, M. Kajino, R. Draxler, M. C. Hort, A. Malo, T. Torii, Y. Sanada. *Atmos. Chem. Phys.* **15**, 1029 (2015), <https://doi.org/10.5194/acp-15-1029-2015>.
- [2] M. Andoh, Y. Nakahara, S. Tsuda, T. Yoshida, N. Matsuda, F. Takahashi, S. Mikami, N. Kinouchi, T. Sato, M. Tanigaki, K. Takamiya, N. Sato, R. Okumura, Y. Uchihori, K. Saito. *J. Environ. Radioact.* **139**, 266 (2015), <https://doi.org/10.1016/j.jenvrad.2014.05.014>.
- [3] Y. Onda, K. Taniguchi, K. Yoshimura, H. Kato, J. Takahashi, Y. Wakiyama, F. Coppin, H. Smith. *Nat. Rev. Earth Environ.* **1**, 644 (2020), <https://doi.org/10.1038/s43017-020-0099-x>.
- [4] Agriculture, Forestry and Fishery Department of Fukushima Prefecture, Statistics of “Forests and Forestry” in Fukushima Prefecture. Ministry of Agriculture, Forestry and Fisheries of Fukushima Prefecture (in Japanese) (2021).
- [5] K. Yoshimura, Y. Onda, A. Sakaguchi, M. Yamamoto, Y. Matsuura. *J. Environ. Radioact.* **139**, 370 (2015), <https://doi.org/10.1016/j.jenvrad.2014.08.021>.
- [6] S. Ueda, H. Hasegawa, H. Kakiuchi, N. Akata, Y. Ohtsuka, S. I. Hisamatsu. *J. Environ. Radioact.* **118**, 96 (2013), <https://doi.org/10.1016/j.jenvrad.2012.11.009>.
- [7] Y. Yamashiki, Y. Onda, H. G. Smith, W. H. Blake, T. Wakahara, Y. Igarashi, Y. Matsuura, K. Yoshimura. *Sci. Rep.* **4**, 3714 (2014), <https://doi.org/10.1038/srep03714>.
- [8] K. Taniguchi, Y. Onda, H. G. Smith, W. Blake, K. Yoshimura, Y. Yamashiki, T. Kuramoto, K. Saito. *Environ. Sci. Technol.* **53**, 12339 (2019), <https://doi.org/10.1021/acs.est.9b02890>.
- [9] T. Niida, Y. Wakiyama, H. Takata, K. Taniguchi, K. Fujita, A. Konoplev. *Sci. Total Environ.* **821**, 153408 (2022), <https://doi.org/10.1016/j.scitotenv.2022.153408>.
- [10] H. Takata, T. Wakiyama, T. Niida, Y. Igarashi, A. Konoplev. *N. Inatomi. Chemosphere.* **281**, 130751 (2021), <https://doi.org/10.1016/j.chemosphere.2021.130751>.

- [11] S. Nagao, M. Kanamori, S. Ochiai, S. Tomihara, K. Fukushi, M. Yamamoto. *Biogeosciences* **10**, 6215 (2013), <https://doi.org/10.5194/bg-10-6215-2013>.
- [12] J. M. Philips, M. A. Russell, D. E. Walling. *Hydrol. Process.* **14**, 2589 (2000), [https://doi.org/10.1002/1099-1085\(20001015\)14:14<2589::aid-hyp94>3.3.co;2-4](https://doi.org/10.1002/1099-1085(20001015)14:14<2589::aid-hyp94>3.3.co;2-4).
- [13] K. Taniguchi, T. Kuramoto, Y. Onda. in *CRIED*, University of Tsukuba, Tsukuba, Japan (2020).
- [14] K. Taniguchi, K. Yoshimura, Y. Onda. in *CRIED*, University of Tsukuba, Tsukuba, Japan (2020).
- [15] Y. Takeuchi, K. Fujita, K. Nasu, A. Irisawa, H. Arai, K. Taniguchi. in *CRIED*, University of Tsukuba, Tsukuba, Japan (2023).
- [16] K. Taniguchi, Y. Onda, H. G. Smith, W. Blake, K. Yoshimura, Y. Yamashiki, T. Kuramoto. *Sci. Data* **7**, 433 (2020), <https://doi.org/10.1038/s41597-020-00774-x>.
- [17] K. Yoshimura, Y. Onda, A. Sakaguchi, M. Yamamoto, Y. Matsuura. *J. Environ. Radioact.* **139**, 370 (2015), <https://doi.org/10.1016/j.jenvrad.2014.08.021>.
- [18] H. Kato, Y. Onda, X. Gao, Y. Sanada, K. Saito. *J. Environ. Radioact.* **210**, 105996 (2019), <https://doi.org/10.1016/j.jenvrad.2019.105996>.
- [19] M. Aoyama, D. Tsumune, Y. Inomata, Y. Tateda. *J. Environ. Radioact.* **217**, 106206 (2020), <https://doi.org/10.1016/j.jenvrad.2020.106206>.
- [20] K. Sakuma, T. Nakanishi, K. Yoshimura, H. Kurikami, K. Nanba, M. Zheleznyak. *J. Environ. Radioact.* **208**, 106041 (2019), <https://doi.org/10.1016/j.jenvrad.2019.106041>.
- [21] K. Osawa, Y. Nonaka, T. Nishimura, K. Tanoi, H. Matsui, M. Mizoguchi, T. Tatsuno. *Anthropocene* **22**, 40 (2018), <https://doi.org/10.1016/j.ancene.2018.04.003>.
- [22] B. Feng, Y. Onda, Y. Wakiyama, K. Taniguchi, A. Hashimoto, Y. Zhang. *Nat Sustainability* **5**, 879 (2022), <https://doi.org/10.1038/s41893-022-00924-6>.
- [23] H. Arai, K. Fujita, H. Yoshita, K. Taniguchi. *Water* **13**, 3021 (2021), <https://doi.org/10.3390/w13213021>.
- [24] G. R. Leidy, R. M. Jenkins. Department of Defense, Department of the Army, Corps of Engineers, Waterways Experiment Station, Environmental Systems Laboratory (1977).
- [25] S. Hayashi, H. Tsuji. *Global Environ. Res.* **24**, 105 (2020).
- [26] U. Sansone, O. V. Voitsekhovitch. ECP No.3, EUR 16529 EN, European Commission, Luxemborg (1996).
- [27] J. E. Brittain, H. E. Bjørnstad, B. Sundblad, R. Saxén. *Freshwater and Estuarine Radioecology*, pp. 87–96, Elsevier, Amsterdam (1997).
- [28] H. Tsuji, H. Funaki, M. Watanabe, S. Hayashi. *Appl. Geochem.* **140**, 105303 (2022), <https://doi.org/10.1016/j.apgeochem.2022.105303>.
- [29] H. Funaki, H. Tsuji, T. Nakanishi, K. Yoshimura, K. Sakuma, S. Hayashi. *Sci. Total Environ.* **812**, 152534 (2022), <https://doi.org/10.1016/j.scitotenv.2021.152534>.

Supplementary Material: This article contains supplementary material (<https://doi.org/10.1515/pac-2023-0802>).